TWO-POINT CORRELATION MEASUREMENTS OF DENSITY FLUCTUATIONS IN THE W7-AS STELLARATOR

N.P.Basse[1,2] & S.Zoletnik[3], M.Saffman[1,4], W.Svendsen[1,2], G.Kocsis[5], M.Endler[6]

[1] *Risø National Laboratory, EURATOM Association, DK-4000 Roskilde, Denmark*
[2] *Niels Bohr Institute, DK-2100 Copenhagen, Denmark*
[3] *CAT-SCIENCE Bt. Detrekő u. 1/b H-1022 Budapest, Hungary*
[4] *Department of Physics, University of Wisconsin, USA*
[5] *KFKI-RMKI P.O.Box 49 H-1525 Budapest, Hungary*
[6] *Max-Planck-Institut für Plasmaphysik, EURATOM Association, D-85748 Garching, Germany*

1.Introduction

Measurements of fluctuations in a wide selection of plasma parameters are essential in order to continue the progress towards an understanding of anomalous transport caused by turbulence. At the W7-AS stellarator, fluctuations in the plasma density are measured by e.g. collective scattering of a CO_2 laser beam on the plasma. We will present a preliminary analysis of experiments performed using this system. The results show evidence of correlated density fluctuations between two separate measurement volumes.

2. Experimental Configuration

A heterodyne collective scattering system (see *Fig. 1*) using a CO_2 laser has been installed on the W7-AS stellarator with the purpose of studying core density fluctuations [1]. Two vertically line integrated measurement volumes (waist radius w of 4 mm) sensitive to identical wavenumbers $k_\perp$ were created in the plasma. The wave vectors were always directed at an angle of 5° with respect to the major radius R in order to be perpendicular to the magnetic field lines in the center of the plasma ($z = 0$) where the beams were focused. The length of the volumes L can be approximated by $\frac{4w}{\theta_s}$.

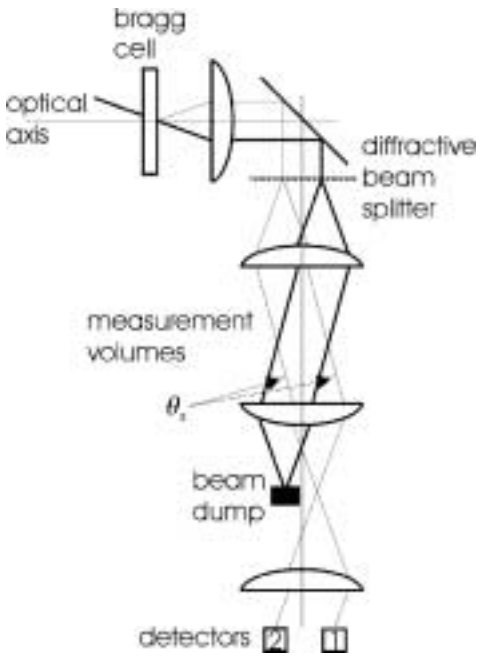

Fig. 1. Schematic representation of the setup [2]; the main beams (M) are represented by thick lines, frequency shifted local oscillator (LO) beams by thin lines. The scattering angle θ_s between the LO and M beams defines the measured $k_\perp$ according to $k_\perp \approx k_{\mathrm{laser}}\theta_s$.

The relative position of these volumes is defined by an angle $\theta_R = \text{Arcsin}\frac{d_R}{d}$, which is the angle between the line connecting the centers of the volumes ($d = 29$ mm) and the φ-axis. **Note:** For the shots analysed in sections 3 and 4, d was 14 mm, w 2 mm. The radial displacement length d_R is directed along the major radius (*Fig. 2*). The angle θ_R can be freely chosen between shots; it is 0° and 90° for toroidally and radially displaced measurement volumes, respectively. θ_R is changed by rotating the diffractive beam splitter.

Fig. 3 shows the vertical line around which the two measurement volumes are rotated (origin of *Fig. 2*). This line is superposed onto the fluxsurfaces; the measurement volumes are centered at 14.5 mm on either side of this line.

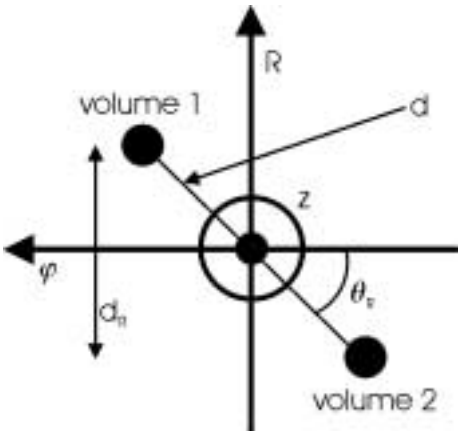

Fig. 2. The rotation of the two measurement volumes. A positive θ_R means that volume 1 is situated at larger R than volume 2.

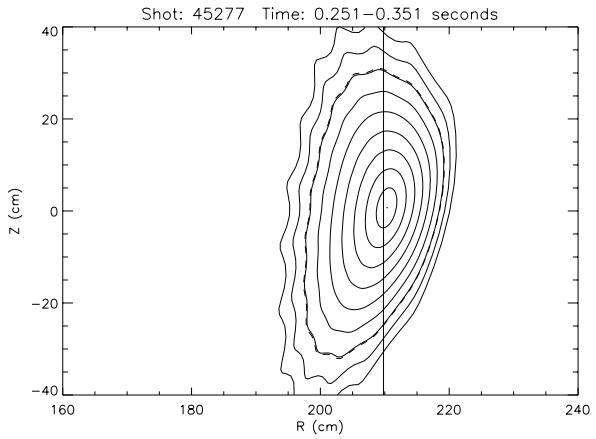

Fig. 3. Poloidal cross section at the toroidal position where the CO_2 diagnostic is situated (toroidal angle $\varphi = 29.14$ °). The dashed line represents the last closed magnetic surface due to limiter action.

The 'pitch angle' of the magnetic field lines in the (φ,R)-plane is defined as $\theta_p = \text{Arctan}\frac{B_R}{B_\varphi}$ (*Fig. 4*). Calculating this angle for the shots considered it is found that this angle varies from 12° at the bottom of the plasma to -4° at the top ($\Delta\theta_p = 16°$). Assuming that the fluctuations are dominated by the perpendicular contribution this implies that the wave vector of the fluctuations changes direction as one moves along a vertical measurement volume. This effect can be exploited to obtain localised measurements, see section 7.

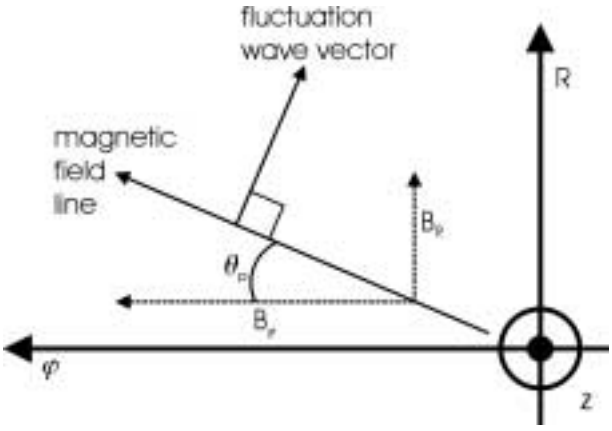

Fig. 4. Field line pitch angle. The fluctuation wave vector is shown as perpendicular to the field line according to the assumption that $k_\parallel \ll k_\perp$.

3. Signal Correlation

Correlation between the two measurement volumes is analysed via crosspower and cross-correlation plots. The normalised crosspower is defined as

$$P_{12}^{n}(\omega) = \frac{F_1^*(\omega)F_2(\omega)}{\sqrt{F_1(\omega)F_1^*(\omega)F_2(\omega)F_2^*(\omega)}},$$

where $F_1(\omega)$ and $F_2(\omega)$ are the Fourier transforms of the two (complex) detector signals. This expression would always yield 1 if the maximum frequency resolution resulting from the digital Fourier transform were used. If one reduces the frequency resolution by binning, the amplitude of the crosspower spectrum is reduced by phase mixing at frequencies where the phase changes randomly. At frequencies where the crosspower spectrum has a definite phase the amplitude stays finite. The complex crosspower spectrum is visualised by plotting the amplitude and the phase as shown in *Fig. 5*.

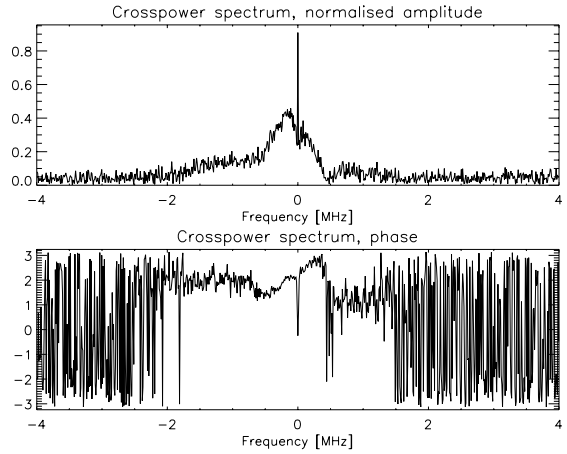

Fig. 5. Normalised crosspower spectrum of the two scattering signals for toroidal alignment (shot 45277, $k_\perp = 40$ cm^{-1}).

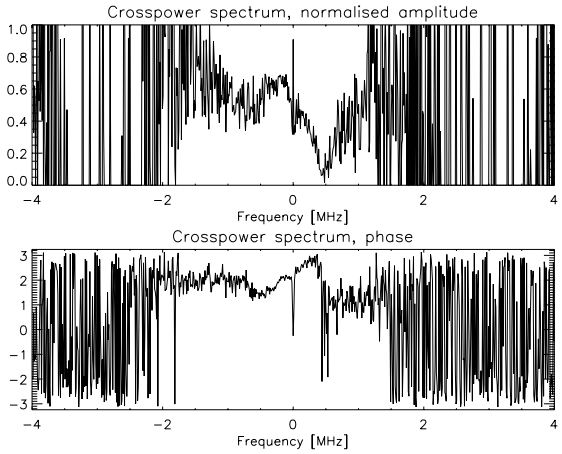

Fig. 6. Normalised, detector noise corrected crosspower spectrum of the two scattering signals for toroidal alignment (shot 45277, $k_\perp = 40$ cm^{-1}).

The spectrum shows a significant nonzero amplitude only if the two channels are aligned within about 20° relative to the local magnetic field direction somewhere along the volume. In this case the crosspower spectrum can be divided into several parts. Above 2 MHz the phase is random and the amplitude is close to zero, thus the signals are not correlated. (Due to the finite sample length the amplitude never falls exactly to zero.) At very low frequencies ($\approx$ 10 kHz) the signals are highly correlated, this region corresponds to fluctuations in the laser power or vibrations of the optical system. Over a range covering a few hundred kHz on both the negative and the positive frequency side of the spectrum one observes a substantial correlation amplitude and a linear phase dependency on the frequency (linear-phase-shift feature). Around 1-2 MHz one observes correlation but with a constant phase at all frequencies (constant-phase feature).

It should be noted that the amplitude of the normalised crosspower spectrum reaches only about 0.4 (disregarding the instrumental peak at 0 Hz), thus a considerable fraction of the signal is uncorrelated. This is partly caused by detector noise because in the normalisation one uses the total signal power which includes detector noise as well. This can be corrected by determining the approximate detector noise power spectrum $n(\omega)$ and subtracting it from the total power at the normalisation:

$$P_{12}^{n,corr}(\omega) = \frac{F_1^*(\omega)F_2(\omega)}{\sqrt{\left[F_1(\omega)F_1^*(\omega) - n_1(\omega)\right]\left[F_2(\omega)F_2^*(\omega) - n_2(\omega)\right]}}$$

Using the above expression one gets irrelevant values for the frequency range where only detector noise is present, but at frequencies where density fluctuations are seen one gets a more realistic approximation of the level of crosscorrelation. As one can see in *Fig. 6* the detector noise corrected crosspower amplitudes reach about 0.6 for both the linear-phase-shift and the constant-phase feature, the low crosspower in the uncorrected plots for the constant-phase feature is the result of the low S/N ratio.

The crosscorrelation function of the two complex detector signals is calculated by correlating the real parts:

$$C_{12}(\tau) = \frac{\int Re\{S_1(t)\}Re\{S_2(t+\tau)\}\mathrm{d}t}{\sqrt{\int Re\{S_1(t)\}^2\mathrm{d}t \int Re\{S_2(t+\tau)\}^2\mathrm{d}t}}$$

An example crosscorrelation function is shown in *Fig. 7.* For this figure the signals were high-pass filtered at 100 kHz and signal powers used in the normalisation were corrected for the detector noise. A negative correlation peak is seen around 0 time lag but significantly shifted towards negative values. The negative peak and the low magnitude of the crosscorrelation can be understood from the crosspower spectrum. As the fluctuation amplitude is largest around 100 kHz (the very low frequency peak is cut by the highpass filter applied before the correlation calculation) one expects the effect of the linear-phase-shift feature to dominate the crosscorrelation function.

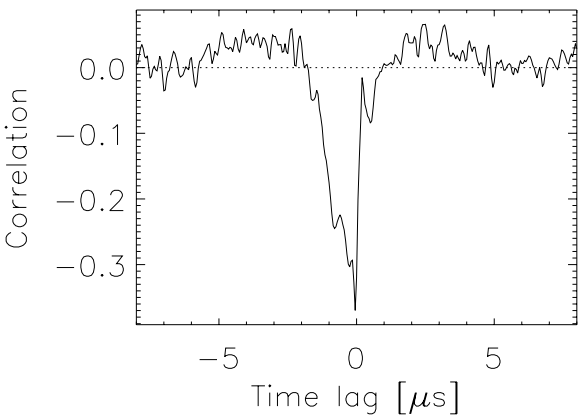

Fig. 7. Crosscorrelation function of the real part of the signals (shot 45277, $k_\perp = 40$ cm^{-1}).

This is indeed the case. It can be shown that a linear phase shift in the crosspower spectrum corresponds to a time delay in the crosscorrelation function. Let $S_1(t)$ and $S_2(t)$ be the two measured signals. If $S_2(t) = S_1(t - \delta t)$, the crosspower spectrum can be written as

$$C(\omega) = \left[\int_{-\infty}^{\infty} S_1(t)e^{-i\omega t}\mathrm{d}t\right]^* \int_{-\infty}^{\infty} S_1(t-\delta t)e^{-i\omega t}\mathrm{d}t = e^{-i\omega\delta t}P_1(\omega),$$

where $P_1(\omega)$ denotes the power spectrum of S_1. As one can see the phase of the crosspower spectrum changes linearly with frequency and the slope is the time delay. It can also be shown that if a fixed phase shift $\delta\phi$ is present between the two signals it will multiply the amplitude of the crosscorrelation function peak by a factor of $\cos(\delta\phi)$. As the linear phase shift curve crosses 0 Hz at about 2 radians and cos(2) = -0.41, the negative sign and relatively low magnitude of the crosscorrelation peak are both a result of a phase shift between the two channels. An arbitrary fixed phase shift is indeed introduced in the optical setup by different optical path lengths in the two channels. The constant phase feature also has a relative phase around 2, thus it would manifest itself as an approximately 0.5-1 μs wide negative peak in the crosscorrelation function at 0 delay. It could be the case that the observed asymmetric shape of the peak in the crosscorrelation is a result of two phenomena. This observation indicates that for the CO_2 laser scattering experiment the crosscorrelation between the two channels can be analysed best using the crosspower spectrum.

4. Previous Experiments

The motivation to do the presented experiments came from two earlier $k_\perp$ scans: One toroidal and one radial. For the case of radial alignment no correlation was seen between the volumes while considerable correlation was observed for toroidal alignment as one would expect if fluctuations are stretched along the field lines (see *Figs. 5 & 8*). This gave us the idea that we could modify the setup so as to allow a shot-by-shot rotation of the measurement volumes. In this fashion, going from toroidal to radial alignment would lead to a falloff of the correlation, thereby giving us an estimate of the radial correlation length (we had already determined that it would be $\leq$ 14 mm).

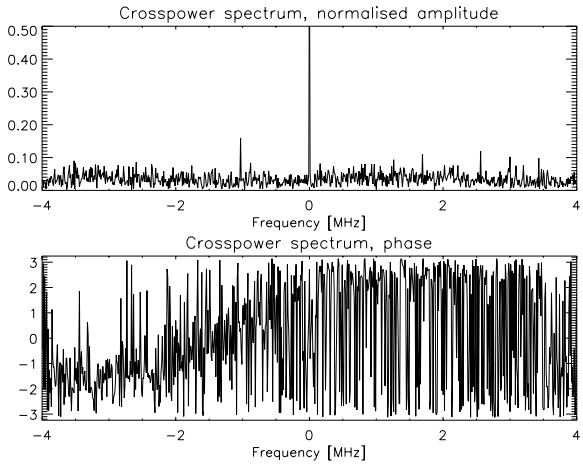

Fig. 8. Normalised crosspower spectrum of the two scattering signals for radial alignment (shot 45232, $k_\perp$ = 54 cm^{-1}).

5. Results

Having understood the meaning of the crosspower spectrum a series of discharges was performed at constant $k_\perp$ = 20 cm^{-1} where we changed θ_R from shot-to-shot.

The shots analysed consisted of two distinct phases: The first phase of about 200 ms duration was steady state, the second transient. We will in this paper limit ourselves to an analysis of the steady-state phase. Further analysis will be presented elsewhere.

The ECRH heated (on-axis, 410 kW) discharges considered here had a flat density profile of 7 $\times$ 10^{19} m^{-3} and a peaked electron temperature profile with a maximum of 1.2 keV. The diamagnetic energy $W_{\rm dia}$ was 10 kJ.

The rotational transform ι was 0.344 which is on the 'good confinement' side of the ι =

0.35 'edge' of the W7-AS device [3].

Crosspower spectra from this series were analysed. The results show clear tendencies (*Fig. 9*). Moving from negative to positive angles relative to the magnetic field direction in the plasma center we see the dominant part of the crosspower amplitude spectrum moving from positive to negative frequencies; that is, the velocity of detected fluctuations relative to the analysing wave vector changes sign. This observation can be understood by assuming fluctuations move poloidally around the magnetic axis and that the crosspower spectrum detects those fluctuations that are localised at a vertical position along the measurement chords where the local magnetic field is directed along the line connecting the two measurement volumes. Furthermore the vertical position corresponds to a particular value of the effective minor radius r_{eff} in the plasma. This way of analysing the crosspower spectrum enables one to localise where the fluctuations come from along the measurement volumes. Keeping this in mind a qualitative radial profile of the absolute magnitude of the electron density fluctuations in the W7-AS stellarator can be found. Both above and below the magnetic axis fluctuations are seen propagating in the same poloidal direction (that is in opposite directions relative to the major radius). In the plasma center the fluctuations have at least a factor of three smaller amplitude (assuming isotropy, i.e. that the poloidal and radial wave vector components are equally weighted) and therefore fall below the detection limit of the current diagnostic setup.

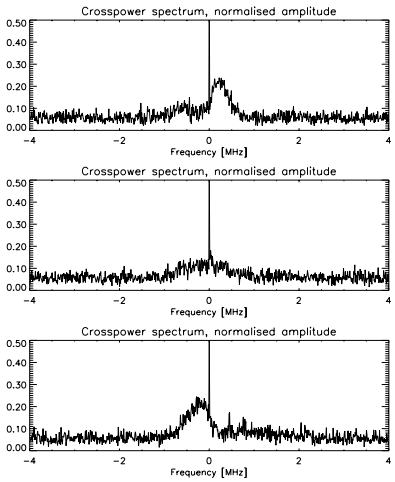

Fig. 9. Normalised crosspower amplitude spectrum of the two scattering signals for three measurement channel alignments ($k_\perp$ = 20 cm^{-1}). Top to bottom: θ_R = -15 °, 0 ° and +20 °.

6. Toroidal Flow Reversal Experiments

A hypothesis from the results described in section 5 was that the observed effects could be due to a unidirectional toroidal flow. To test this idea, shots were made with co - and counter (direction of beam-driven current w.r.t. the bootstrap current) neutral beam injection (NBI) to impart toroidal momentum of opposite direction to the bulk plasma.

The shots were made as similar as possible to the ECRH shots, the NBI power was 500 kW and other parameters were identical except ι which was changed to 0.349.

Figs. 10 and *11* show crosspower plots of shots having identical experimental parameters; only the beam direction was changed. This leads to a difference in W_{dia} due to the fact that counter beam heating creates a broader deposition profile.

An obvious feature when comparing the Figures is that the correlation is generally larger for the counter-injection case. One would be tempted to suggest that this connects to the fact that $W_{\mathrm{dia,co}} \geq W_{\mathrm{dia,cntr}}$; however, this doesn't hold if one analyses a large selection of discharge types.

Comparable are the linear-phase-shift feature from -2 MHz to -500 kHz and the constant-phase feature at low positive frequencies ([100,600] kHz). The counter-shot has an additional low frequency linear-phase-shift feature from -500 to -100 kHz.

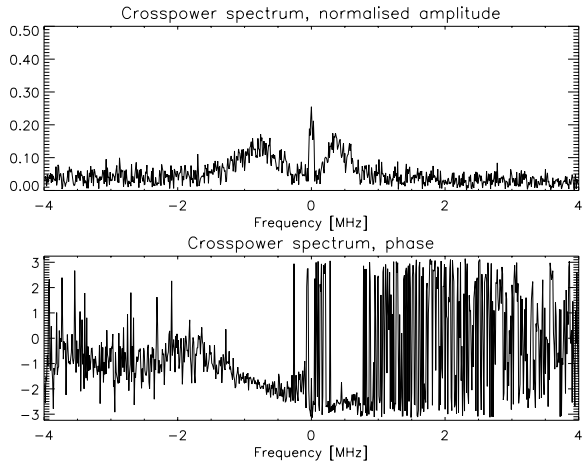

Fig. 10. Normalised crosspower, shot 48094 (θ_R = -9.5 °, $k_\perp$ = 15 cm^{-1}), co-injection.

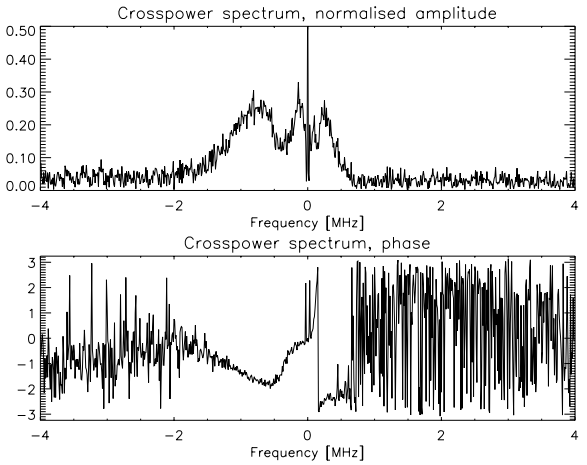

Fig. 11. Normalised crosspower, shot 48096 (θ_R = -9.5 °, $k_\perp$ = 15 cm^{-1}), counter-injection.

To conclude, there are certainly large differences in the correlation of density fluctuations for co- and counter-NBI heated discharges, but not to the effect that features change frequency sign.

7. Magnetic localisation

To obtain localised measurements we adopted a technique developed by the ALTAIR team at the TORE SUPRA tokamak [4].

The 'angular resolution' $\Delta\alpha_{k_\perp} = \frac{\Delta k_\perp}{k_\perp}$ is a measure of how large an angle around the selected measurement direction we get a scattered signal from. The 'wavenumber resolution' $\Delta k_\perp$ is equal to $\frac{2}{w}$, where w is the waist of the beams in the plasma center. The requirement for localisation is that $\Delta\alpha_{k_\perp} \ll \Delta\theta_p$.

In section 2 we mentioned that our measurements are line integrated along vertical chords. The reason for this can be explained as follows: In the experiments described herein the beam waist was 4 mm; choosing $k_\perp$ to be 20 cm^{-1} we get an angular resolution of 14.3°.

We went from a two to a one-beam setup and made the waist of this beam quite large (w = 33 mm) to get a $\Delta\alpha_{k_\perp}$ of 2.3° for $k_\perp$ = 15 cm^{-1}.

A series of 6 identical shots was made where we changed the horizontal direction of $k_\perp$ from shot-to-shot. Shown in *Figs. 12 & 13* are measurements of the total scattered power in a frequency band from this scan ($k_\perp$ = 15 cm^{-1}) vs. time. Colours from the bottom to the top of the plasma along the measurement volumes are: Black, dark blue, red, light blue, green and yellow.

In the steady-state phase considered here (200 to 400 ms in the Figures), it is clearly seen that the fluctuation amplitude in the two central volumes (red and light blue) is quite low

compared to other volumes. This observation hints towards the conclusion that the density fluctuations are events localised as poloidally moving in an outer band of r_{eff}.

The large spikes at some positions in the steady-state phase are not understood at present.

Turning to the outer volumes it is first of all seen that the fluctuation amplitude is considerably larger than in the core plasma. This correlates very well with the findings reported in section 5.

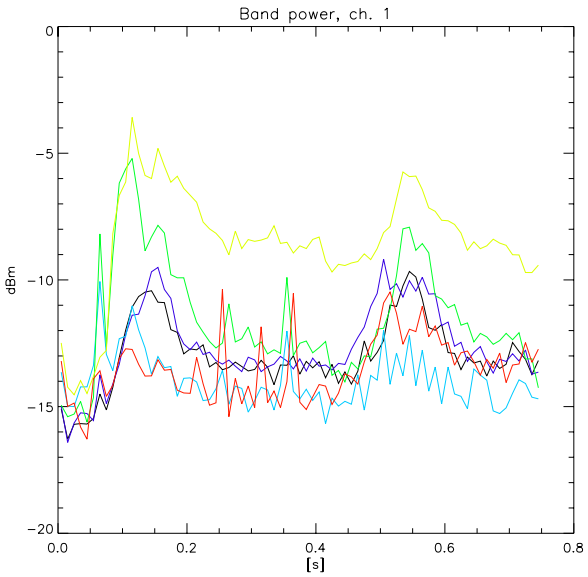

Fig. 12. Scattered power in the [100,200] kHz interval.

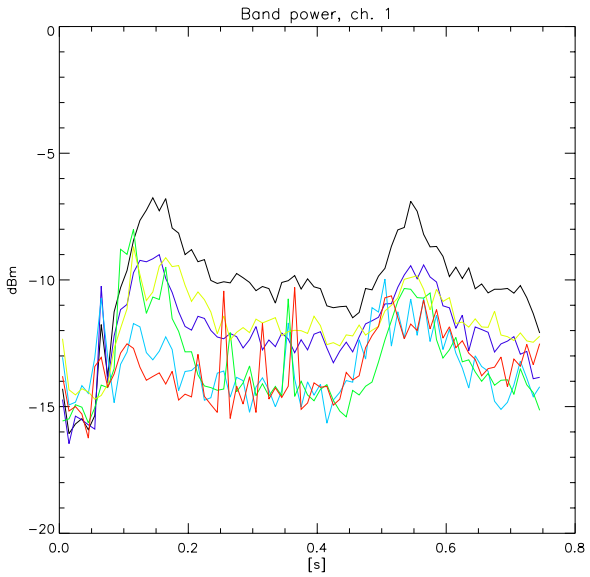

Fig. 13. Scattered power in the [-200,-100] kHz interval.

8.Conclusions

We have in this paper presented two ways of obtaining spatial localisation of density fluctuations along our measurement volumes:

- In the first method one broad measurement volume was used which results in a good wavenumber resolution. Using the fact that the magnetic field direction changes along the observation volume and assuming $k_{\|} = 0$ for the fluctuations one measures fluctuations originating in a small vertical region as was shown in [4].
- The second way by a novel concept: Assuming that the fluctuations are stretched along the field lines and have a cross-field correlation of less than about 1 cm, the crosspower of the two signals contains a contribution only from those volumes where the local magnetic field is aligned approximately along the measurement volumes.

Using both techniques we came to the qualitative result that fluctuations in the central region of the plasma have a much smaller amplitude than fluctuations in the outer parts.

To understand the interplay between the magnetic field and our measurements we are presently implementing a simulation trying to take the various effects into account. We think this is necessary in order to further quantify the results reported in this paper.

[1] S.Zoletnik et al., 26^{th} EPS, Maastricht, **ECA 23J** 1493 (1999).
[2] N.P.Heinemeier, Risø Report R-1064(EN) (1998).
[3] R.Brakel et al., Plasma Phys. Control. Fusion **39** B273-B286 (1998).
[4] A.Truc et al., Rev. Sci. Instrum. **63** (7) (1992).